

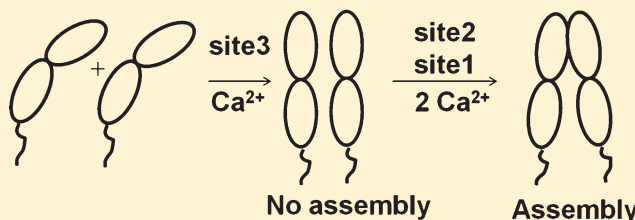
Sequential Binding of Calcium Leads to Dimerization in Neural Cadherin

Nagamani Vunnam and Susan Pedigo*

Department of Chemistry and Biochemistry, University of Mississippi, University, Mississippi 38677, United States

S Supporting Information

ABSTRACT: Neural cadherin (N-cadherin) is a calcium-dependent homophilic cell-adhesive molecule and critical for synaptogenesis and synapse maintenance. The extracellular region plays an important role in cadherin-mediated cell adhesion and has five tandemly repeated ectodomains (EC1–EC5) with three calcium-binding sites situated between each of these domains. Adhesive dimer formation is significantly dependent on binding of calcium such that mutations in the calcium-binding sites adversely affect cell adhesion. To investigate the relative significance of the calcium-binding sites at the EC1–EC2 interface in calcium-induced dimerization, we mutated three important amino acids, D134, D136, and D103, in NCAD12, a construct containing EC1 and EC2. Spectroscopic and chromatographic experiments showed that all three mutations affected calcium binding and dimerization. Mutation of D134, a bidentate chelator in site 3, severely impaired the binding of calcium to all three sites. These findings confirm that binding to site 3 is required for binding to occur at site 2 and site 1. Interestingly, while the D103A mutation diminished only the affinity for calcium, it completely eliminated dimerization. Equilibrium dialysis experiments showed a stoichiometry of 3 at 2 mM calcium for D103A, but no dimerization was apparent even at 10 mM calcium. These results indicate that calcium binding alone is not sufficient for dimerization but requires cooperativity between calcium-binding sites. In summary, our findings confirm that the calcium-binding sites are occupied sequentially in the order of site 3, then site 2 and site 1, and that cooperativity between site 2 and site 1 is essential for formation of adhesive dimers by N-cadherin.



Cadherins are calcium-dependent cell adhesion proteins that mediate cell–cell adhesion through interactions with cadherins on neighboring cells.^{1–5} Type I or classical cadherins are located in adherens junctions and are named according to the cell type in which they predominate.^{6,7} Cadherins mediate dynamic cellular processes during embryogenesis, tissue morphogenesis,^{8,9} and cell differentiation.¹⁰ Cadherins are critical for regulating the reorganization of adult soft tissues.¹¹ Abnormal cadherin expression, molecular defects in cadherin function, and mutations in calcium-binding sites are associated with metastatic cancers.^{12–14} The studies reported here address the linkage between calcium binding and dimerization in neural cadherin.

Neural cadherin (N-cadherin) plays an important role in the development of the nervous system during embryogenesis.¹⁵ N-Cadherin is critical for synaptogenesis and synapse maintenance.^{16,17} It optimizes synaptic function via the constant regulation of synaptic plasticity.^{18,19} Altered metabolism of N-cadherin results in synaptic dysfunction, a primary feature of Alzheimer's disease.²⁰ Abnormal expression of N-cadherin by cancer cells can contribute to invasiveness and metastasis by making the cells more motile.^{21–23}

Classical cadherins have a common domain organization.^{6,7,24} The primary structure of cadherins comprises an extracellular (EC) region, a single-pass transmembrane region, and a conserved cytoplasmic region, which interacts with the actin cytoskeleton through catenins.^{25–28} The EC region has five tandemly

repeated EC domains (EC1–EC5) with three calcium-binding sites at the interface between adjacent EC domains. A high-resolution structure of EC1–EC5 showed that all calcium-binding sites are organized similarly.²⁹ Cell aggregation studies established that cadherin-mediated cell–cell adhesion requires calcium binding.^{28,30–32} Binding of calcium links the modular domains to create a cooperative unit that signals adhesion to the cytoplasm of the cell.³³ Electron microscopy of the EC domains showed that the binding of calcium leads to a rigid curved shape, whereas in the absence of calcium, the structure collapses to a more compact form,^{34,35} which has an increased susceptibility to proteolysis.³¹ Mutation of the calcium binding amino acid, D134, abolishes cadherin function and increases susceptibility to proteolysis.⁵ Through bead aggregation and atomic force measurements, Prakasam et al.³⁶ showed that disruption of the amino acids at calcium-binding sites can abolish cadherin-mediated cell adhesion. This was also predicted in molecular dynamic simulations.^{37,38}

Recent studies illustrate the significance of the EC1 domain in cadherin-mediated cell–cell adhesion.^{39,40} Nuclear magnetic resonance (NMR)^{41,42} and X-ray crystallography^{29,43–45} have shown that neighboring cadherins dimerize through their

Received: November 23, 2010

Revised: February 28, 2011

Published: March 02, 2011

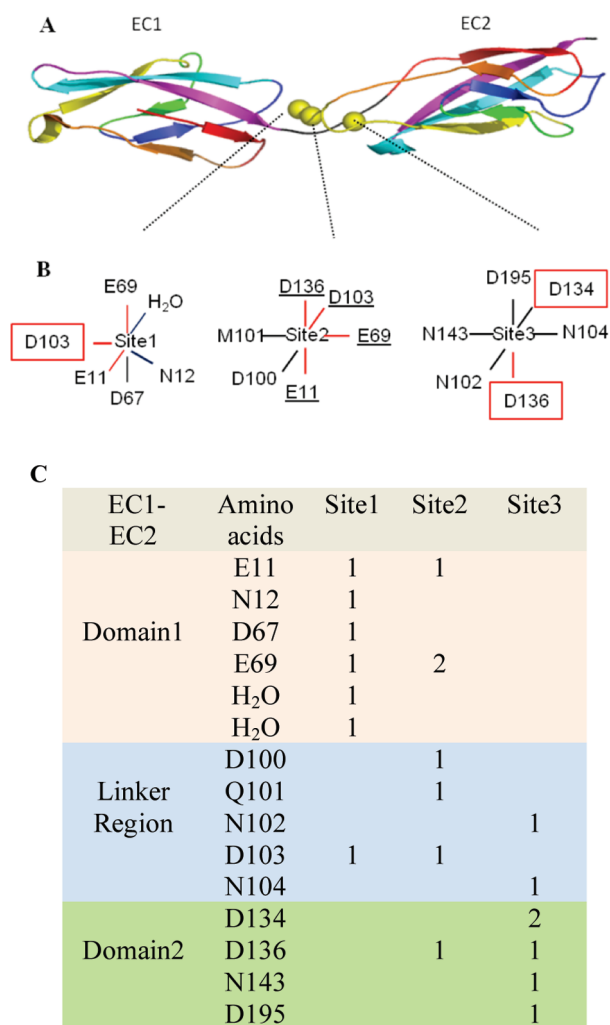


Figure 1. Details of calcium-binding sites. (A) Ribbon drawing of EC1 and EC2 of E-cadherin produced from the crystal structure of Nagar et al.⁵⁴ (B) Chelating amino acids in the calcium-binding sites at the EC1–EC2 interface. The underlined amino acids and D134 are bidentate chelators. We have mutated the amino acids in the red boxes. (C) Summary of calcium-binding amino acids at the EC1–EC2 interface. A survey of the crystal structures of the first two domains (EC1 and EC2) of E- and N-cadherins showed heterogeneity in calcium-binding sites.^{43,53,54} Because calcium-binding pockets are organized similarly in E- and N-cadherins, we have used PDB entry 1FF5⁵³ to identify the calcium-chelating amino acid at the EC1–EC2 interface. All three calcium-binding sites are chelated by seven oxygen atoms and are linked by four bridging amino acids (E11, E69, D103, and D136). The numeral 1 indicates monodentate coordination and the numeral 2 bidentate coordination.

N-terminal EC1 domains. Structural^{29,44,46} and antibody interaction studies⁴⁷ suggest that the binding of calcium ions induces a conformational change in EC1 by undocking the conserved tryptophan 2 (W2) from its own hydrophobic pocket and docking it into the hydrophobic pocket of its adhesive partner, which leads to cell–cell adhesion. Mutations in the key calcium binding residues, DXD (D134 × D136), markedly decreased the extent of adhesion.^{5,13,48,49} Thus, proper binding of calcium at the interfaces between the domains is critical for cell–cell adhesion and is an important issue with regard to cadherin function. The calcium binding affinity for the EC1–EC2 and

EC1–EC5 constructs of epithelial cadherin has been estimated by different groups using a variety of methods,^{34,35,50,51} but the order of occupancy and the relative significance of each binding event are not known.

We have focused our studies on the three calcium-binding sites at the EC1–EC2 interface (Figure 1A). Calcium-binding sites are composed of clusters of negatively charged residues or carbonyl groups from the loops that connect the β -sheet regions within the individual domains and the linker peptide that connects one domain to the next. Amino acids at the interface of the first two domains play an essential role in adhesion.⁵² These amino acids comprise three calcium-binding sites that are labeled as sites 1–3 (Figure 1C). It is not known which site binds first, and there is no consensus binding motif. All three calcium-binding sites are coordinated by seven oxygen atoms⁵³ (Figure 1B). Binding site 1 and site 2 are connected by three bridging amino acids, E11, E69, and D103.^{53,54} Each of these amino acids donates one side chain oxygen to site 1 and the other to site 2, thereby linking these two calcium-binding sites. D134 provides both of its side chain oxygens to site 3. Further, site 2 and site 3 are linked by D136, which provides one side chain oxygen to site 2 and the other side chain oxygen to site 3.

In spite of extensive studies, the molecular details of calcium-induced formation of adhesive dimers are not well understood. The relative significance of the calcium-binding sites at the EC1–EC2 interface in calcium-induced dimerization is not known. How does a point mutation in amino acids in site 3 at the EC1–EC2 interface abolish the adhesive property of cadherins? Is binding of calcium sequential such that binding to site 3 is the key step in the formation of the adhesive dimer?

To address these questions, we mutated critical amino acids in the calcium-binding sites at the EC1–EC2 interface. Mutation of D134 addresses sequential binding by targeting calcium binding to site 3 in particular. Mutation of D136 was designed to address the significance of the linkage between site 3 and site 2. Mutation of D103 addresses the importance of the linkage between site 2 and site 1. Spectroscopic and chromatographic experiments were used to determine the impact of calcium-binding site mutations, D103A, D134A, and D136N, on stability, calcium binding affinity, and calcium-induced dimerization. These studies show that calcium binding is sequential and linkage between calcium-binding sites is critical for dimerization of N-cadherin.

EXPERIMENTAL PROCEDURES

Site-Directed Mutagenesis. The cDNA of mouse N-cadherin was provided by L. Shapiro (Columbia University, New York, NY) and was used as a template for PCR amplification of the gene for the first two ectodomains (residues 1–221), designated as NCAD12 (NCAD12 consisting of EC1, linker 1, EC2, and linker 2). The plasmid construct encoding the first two EC domains of N-cadherin was cloned into a pET30 vector using the Xa/LIC system (Novagen). Amplification of the two-domain constructs, digestion of template DNA with restriction enzymes, ligation of the fragments into the pET30 Xa/LIC expression vector, and subsequent transformation into *Escherichia coli* BL21(DE3) expression cells were performed according to standard protocols, utilizing KOD HiFi DNA Polymerase (Stratagene). Point mutations were introduced into the NCAD12 sequence by site-directed mutagenesis by using the Quickchange kit (Stratagene) with the following sense primers: D134A, 5' CGG TCA CTG CCA TTG CCG CGG ATG ATC

CAA ATG CCC 3'; D136N, 5' GCC ATT GAT GCG AAT GAT CCA AAT GCC C 3'; and D103A, 5' GAC ATG AAT GCG AAC AGA CCT GAG TTT CTG CAC 3'. Point mutations were confirmed by sequencing the resultant plasmids.

Overexpression and Purification. For production of NCAD12-WT (wild-type), NCAD12-D134A (D134A), NCAD12-D136N (D136N), and NCAD12-D103A (D103A), 2000 mL of Luria-Bertani broth with 30 $\mu\text{g}/\text{mL}$ kanamycin was inoculated with a transformed colony picked from an agar plate. Cultures were grown at 37 °C to an OD₆₀₀ of ~0.8–1.0 and then induced via the addition of 0.4 mM IPTG. Two hours post-induction, cells were harvested by centrifugation. Pellets were suspended in buffer, frozen, thawed, lysed by sonification, and centrifuged. Proteins were found in the inclusion bodies. Insoluble protein was separated from membrane components by washing with dilute solutions of Triton X-100. Pellets were suspended in denaturing His Tag binding buffer [6 M urea, 20 mM Tris-HCl, 0.5 M NaCl, and 5 mM imidazole (pH 7.5)]. Supernatants were applied to a Ni affinity column (Amersham) and washed with 20 mM Tris-HCl, 500 mM NaCl, and 0.04 M imidazole (pH 7.9). The proteins were eluted with 10 mM Tris-HCl, 250 mM NaCl, and 0.5 M imidazole (pH 7.9) at 25 °C. The elution fractions containing protein were dialyzed in 140 mM NaCl, 20 mM Tris, 10 mM CaCl₂, 1 mM DTT, and 5% glycerol (pH 7.4). Immobilized trypsin (Pierce) was used to remove the 45-residue N-terminal affinity label. The digestion mixture (500 μL protein/250 μL of immobilized trypsin) was incubated with rapid shaking for 5 h at 25 °C and centrifuged. The supernatant was dialyzed against 140 mM NaCl and 10 mM HEPES (pH 7.4) to remove calcium ions and cleaved peptide. The digested proteins were further purified and buffer exchanged using size exclusion chromatography (SEC) using a Sephacryl S-100 (Amersham) 1.2 cm \times 0.5 m (~100 mL) column in 140 mM NaCl and 10 mM HEPES (pH 7.4). The residual level of calcium in the SEC buffer was found to be <1 μM by inductively coupled plasma optical emission spectroscopy (ICP-OES). The purity of the proteins was assessed by sodium dodecyl sulfate–polyacrylamide gel electrophoresis in 17% polyacrylamide gels. The extinction coefficients were determined experimentally on the basis of the amino acid composition using a molar absorption coefficient of tryptophan and tyrosine residues in the denatured state using the method of Edelhoch.⁵⁵ The following extinction coefficients at 280 nm were used: 17700 \pm 500 M⁻¹ cm⁻¹ for the wild type, 16600 \pm 700 M⁻¹ cm⁻¹ for D134A, 16800 \pm 400 M⁻¹ cm⁻¹ for D136N, and 16600 \pm 250 M⁻¹ cm⁻¹ for D103A. Protein concentrations were determined spectrophotometrically using these extinction coefficients.

Spectral Characterization. UV spectra were recorded on a Cary 50 Bio UV–vis spectrophotometer in a 1 cm quartz cuvette from 350 to 200 nm at room temperature. Circular dichroism (CD) spectra were recorded on an Aviv model 202SF CD spectrometer using a 0.5 mm path length cuvette with a 5 s averaging time at 25 °C. The spectral changes were monitored in the presence and absence of calcium. To confirm that the apoprotein stocks were free of calcium, spectral studies were also performed with 5 mM EGTA added. The protein solutions (60 μM) were scanned from 200 to 300 nm at rate of 1 nm/s. All spectral data were corrected for buffer signal, in 140 mM NaCl and 10 mM HEPES (pH 7.4).

Thermal Unfolding Studies. Thermal unfolding of the wild type, D134A, D136N, and D103A was monitored with an AVIV 202SF CD spectrometer. The temperature was varied from 15 to

80 °C. All experiments were performed using a quartz cuvette with a 1 cm path length fitted with a screw top through which the temperature probe was inserted. The temperature ramp rate was 1 °C/min with a 30 s to 1 min equilibration and a 5 s acquisition time at 230 nm. To observe the effect of calcium binding, we performed studies at two calcium concentrations, the apo state (5 mM EGTA) in 140 mM NaCl and 10 mM HEPES (pH 7.4) and the saturated state with 1 mM calcium added. At high calcium concentrations (5 and 10 mM), proteins precipitated during the thermal denaturation experiments. The thermal unfolding transitions were fit to the Gibbs–Helmholtz equation with linear native and denatured baselines with adjustable slopes and intercepts as described previously.⁵⁶ The ΔC_p for apo-NCAD12 was determined experimentally by a series of temperature denaturation experiments in the presence of urea at concentrations of 0, 0.2, 0.4, 0.6, and 0.8 M for the apo conditions (140 mM NaCl, 2 mM HEPES, 1 mM TCEP, and 10 μM EGTA) and found to be 1 kcal mol⁻¹ K⁻¹. The value for ΔC_p was resolved from the Kirchoff plot of the observed enthalpy of denaturation versus transition temperature (data not shown).

Calcium Binding Studies. Direct calcium titrations were monitored by CD and fluorescence emission (FL) spectroscopy. The titrations were performed on 2.5 μM protein solutions in 140 mM NaCl and 10 mM HEPES (pH 7.4) at 25 °C. The titrations monitored by CD were conducted in a 0.4 cm \times 1 cm cuvette with stirring by addition of small volumes (2, 5, or 10 μL) of calcium chloride stocks at different concentrations (1 mM, 10 mM, 100 mM, and 0.7 M). After each addition of calcium, a spectrum was recorded from 220 to 300 nm. Each titration was performed in triplicate. The spectra were corrected for offset differences. CD data at wavelengths between 227 and 235 nm were analyzed as individual titration curves. The total calcium concentration was assumed to be equivalent to the free calcium concentration because the protein concentration was low. Calcium titrations were also monitored by FL. The protein solutions were titrated in a fashion identical to that described above. Emission spectra were recorded from 300 to 425 nm with the excitation wavelength set at 290 nm.

The calcium titration data were fitted to a model of equal and independent binding shown in eq 1

$$\bar{Y} = \frac{K_a X}{1 + K_a X} \quad (1)$$

where \bar{Y} is the fractional saturation of sites and K_a is the calcium association constant.

To accommodate the experimental data without prior normalization, the function used for fitting the data is shown in eq 2

$$F(X) = \text{baseline}_{\text{apo}} + \bar{Y} \times \text{span} \quad (2)$$

where the apo and saturated baselines are linear functions and the span is the difference between them.

The spectral signal of the sample before calcium was added was assigned a free calcium concentration on the basis of results from ICP-OES. Analysis of these spectroscopic data provides information regarding only the midpoint, not the stoichiometry, of calcium binding. Residuals to the fits to eq 2 were random, indicating that the data did not support analysis by a more complex model. Titrations monitored by CD had baseline slopes of zero. The span of the transition in the titrations monitored by FL was small (only 5% of the signal) such that the slight slope in the baseline was significant. Thus, to resolve the midpoint of the

transitions monitored by FL, we allowed the slope to vary in these fits.

Equilibrium Dialysis Studies. The stoichiometry of calcium binding was determined by equilibrium dialysis using a rapid equilibrium dialysis device (Thermo Scientific). This device contained two chambers (protein and buffer chambers) separated by a thin dialysis membrane (molecular mass cutoff of 8 kDa). A 100 μL volume of the protein sample was added to the protein chamber and was dialyzed against 300 μL of standard buffer [10 mM HEPES and 140 mM NaCl (pH 7.4)] containing varying concentrations of cold Ca^{2+} (0.05–3 mM). To these standard buffer solutions was added 10 $\mu\text{Ci/mL}$ of $^{45}\text{Ca}^{2+}$ (PerkinElmer). Total calcium concentrations were corrected to account for this addition. The base plate was incubated at room temperature (23 $^{\circ}\text{C}$) with continuous agitation. A 95 μL volume of sample from protein and buffer chambers was mixed with 5 mL of scintillant. The radioactivity was determined in a liquid scintillation spectrometer. To determine the time required for the equilibration, protein and buffer samples were counted after 8, 12, 14, and 16 h. The radioactivity counts observed at the 14 and 16 h incubation times were identical, confirming that equilibrium was achieved after equilibration for 14 h. From the measured radioactivity counts, the moles of bound calcium per mole of protein and the free calcium concentration were determined. Protein concentrations used in this experiment ranged from 50 to 500 μM depending on the Ca^{2+} concentration. High protein concentrations were essential for obtaining reasonable saturation values at high total Ca^{2+} concentrations.

The resulting data were fit to eq 3 to resolve the stoichiometry of calcium binding

$$\bar{v} = n \frac{K_a X}{1 + K_a X} \quad (3)$$

where \bar{v} is the saturation of calcium-binding sites, n is the stoichiometry, K_a is the average binding affinity, and X is the free calcium concentration. While this model allows for an estimate of stoichiometry, data were significantly more cooperative than what this model can accommodate. To resolve estimates of calcium affinity and cooperativity, we fit data to the Hill equation as shown in eq 4

$$\bar{v} = 3 / (1 + X^{-n_H} \times 10^{-b}) \quad (4)$$

where n_H is the Hill coefficient and b is a constant. The calcium binding affinity was the x -intercept of the linear form of this function.

Assembly Studies. Analytical size exclusion chromatography (SEC) was used to indicate the presence of dimer in protein stocks. SEC was performed with a Superose-12 10/300 GL column (Amersham) using an ÄKTA Purifier HPLC system with UV absorbance detection at 280 nm. The mobile phase consisted of 140 mM NaCl and 10 mM HEPES (pH 7.4) with a flow rate of 0.5 mL/min. To observe the effect of calcium on dimerization, we added calcium to the protein stocks but not to the mobile phase. The injection volume was 50 μL , and the protein concentration was 50 μM . The SEC column was calibrated on the basis of the Stokes radius of the standard proteins, human serum albumin, ovalbumin, myoglobin, and cytochrome *c*. Monomeric and dimeric cadherin species were unambiguously identified on the basis of their calculated Stokes radii using monomer and dimer structures from PDB entry

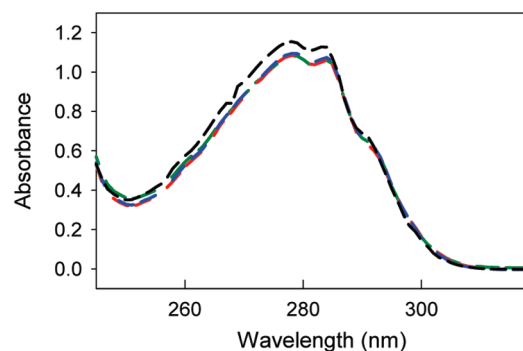


Figure 2. UV spectra of wild-type (black), D134A (green), D136N (red), and D103A (blue) proteins at a protein concentration of 60 μM .

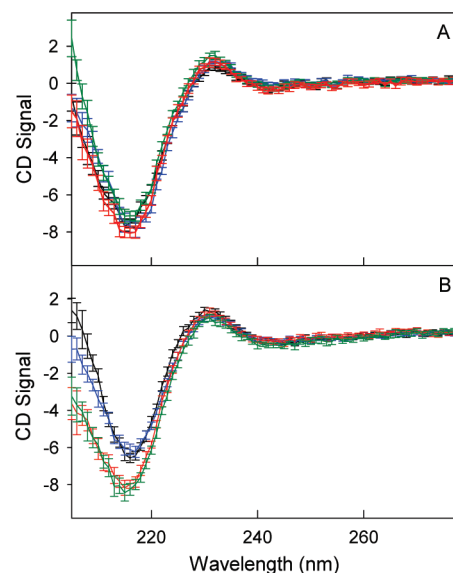


Figure 3. CD spectra of wild-type, D134A, D136N, and D103A proteins. (A) CD spectra of 60 μM wild type (black), D134A (green), D136N (red), and D103A (blue) with 10 μM EGTA (apo). (B) CD spectra of 60 μM wild type (black), D134A (green), D136N (red), and D103A (blue) with 1 mM calcium.

1edh⁵⁴ using HYDROPRO.⁵⁷ We monitored the level of monomer and dimer as the height of the peaks detected at 280 nm.

RESULTS

Spectral Characterization. The UV spectra of the purified wild type, D134A, D136N, and D103A exhibited a local maximum at 280 nm with a shoulder at 290 nm, which is typical of folded proteins that contain tyrosine and tryptophan (Figure 2). All three mutant proteins, D103A, D134A, and D136N, had similar UV spectra and extinction coefficients. The wild-type protein had a greater extinction coefficient and, therefore, higher absorbance than the mutants. These results indicate that the mutations cause a slight change in the environment of the aromatic amino acids in the proteins.

Circular dichroism spectroscopy was used to investigate structural changes in wild-type and mutant proteins as a function of calcium. The CD spectra in the presence and absence of calcium had a wavelength minimum at approximately 218 nm (Figure 3), which is typical for β -sheet proteins.⁵⁸ The CD

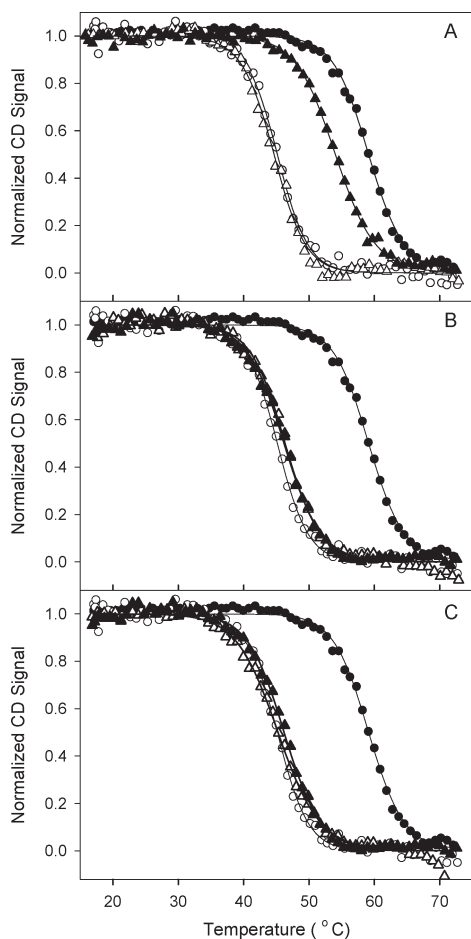


Figure 4. Thermal unfolding of wild-type, D134A, D136N, and D103A proteins. Normalized CD signal vs temperature in the presence (\blacktriangle) and absence (\triangle) of calcium at $5 \mu\text{M}$ protein for (A) D103A, (B) D134A, and (C) D136N. For comparison, results for the wild type in the apo state (\circ) and with 1 mM calcium (\bullet) are shown.

spectra of the wild type, D134A, D136N, and D103A in the apo state were identical, which indicates the point mutations did not change the secondary structure of the proteins (Figure 3A). Upon addition of calcium (1 mM), similar spectral changes were observed for the wild type and D103A (Figure 3B), which implies that D103A binds calcium and that there is similar calcium-dependent conformational change in these two proteins. In contrast, there were no spectral changes with calcium addition in D134A and D136N (Figure 3B), which indicates that the mutations reduce the calcium binding affinity or there is no spectral signal change associated with calcium binding to these proteins.

Thermal Unfolding Studies. Thermal unfolding was monitored by CD spectroscopy at low protein concentrations. Results from the thermal unfolding experiments are summarized in Figure 4. All data were fit to a two-state model according to the Gibbs–Helmholtz equation providing estimates for T_m and ΔH_m . (The value of ΔC_p was fixed to $1 \text{ kcal K}^{-1} \text{ mol}^{-1}$.) In the apo state, all four proteins, wild type, D134A, D136N, and D103A, unfolded with apparent two-state transitions, with similar melting temperatures, enthalpy changes, and free energy changes at 25°C (Table 1). These results indicate that the D134A, D136N, and D103A mutations did not affect the stability of the apoproteins.

Table 1. Summary of Parameters Resolved from Thermal Unfolding Experiments for the Wild Type and Mutants in the Absence and Presence of Calcium

protein	buffer	ΔH_m^a (kcal/mol)	T_m ($^\circ\text{C}$)	ΔG^{ob} (kcal/mol)
wild type	apo	68 ± 8	45 ± 2	3.6 ± 0.5
	Ca^{2+}	79 ± 5	59 ± 3	6.3 ± 0.7
D103A	apo	64 ± 4	46 ± 1	3.5 ± 0.1
	Ca^{2+}	80 ± 4	52 ± 1	5.5 ± 0.2
D134A	apo	61 ± 2	46 ± 1	3.3 ± 0.3
	Ca^{2+}	65 ± 1	46 ± 1	3.6 ± 0.1
D136N	apo	59 ± 2	46 ± 1	3.2 ± 0.2
	Ca^{2+}	60 ± 2	48 ± 1	3.5 ± 0.1

^aThe value of ΔC_p was fixed to $1 \text{ kcal mol}^{-1} \text{ K}^{-1}$. Values are averages and standard deviations of at least three determinations for each parameter. ^b ΔG° is the calculated value of the free energy change upon unfolding at 25°C .

In the presence of calcium (1 mM), the three mutants had a stability lower than the wild-type value (Table 1). Both wild type and D103A exhibited significant increases in T_m and ΔG° upon addition of 1 mM calcium (Figure 4A). However, the smaller increase in T_m and ΔG° in D103A indicates that it binds calcium, but with an affinity lower than that of the wild type. Addition of 1 mM calcium did not significantly stabilize D134A and D136N, such that parameters resolved for both proteins in the absence and presence of calcium are similar (Figure 4B,C). We observed an increase in the melting temperature ($\sim 7^\circ\text{C}$) for both mutant proteins at 10 mM calcium but could not evaluate the data because of the precipitation at high temperatures. The enthalpy change of unfolding was increased upon addition of calcium for D103A and the wild type but remained unchanged for D134A and D136N. Hence, with the binding of calcium, the melting transitions of the wild type and D103A progressed toward higher values of T_m and ΔH_m . This was not observed in the D134A and D136N mutants and provides additional evidence that these mutations significantly impact calcium binding affinity.

Calcium Binding Studies. The calcium-dependent changes in CD and FL spectra were monitored during calcium titrations for all four proteins (wild type, D103A, D134A, and D136N). D134A and D136N showed no CD signal change in calcium titrations. The FL signal from D134A and D136N decreased over the titration but did not reveal behavior consistent with titratable calcium-binding sites (data not shown). These results are consistent with the spectral and thermal unfolding data for D134A and D136N. The CD spectral, thermal denaturation, and calcium binding studies all indicate that these mutations severely impacted calcium binding affinity.

The most striking result is that the calcium titrations monitored by CD (Figure 5A) and FL (Figure 5B) are identical for the wild type and D103A. This is interesting because the thermal denaturation studies show that the D103A mutation impacted the calcium binding affinity. The free energies resolved from the calcium titrations monitored by CD and FL are different (Table 2). Calcium titrations monitored by CD yielded a titration curve with a midpoint of $28 \pm 9 \mu\text{M}$ for the wild type and $40 \pm 20 \mu\text{M}$ for D103A. Titrations monitored by FL yielded a midpoint of $110 \pm 60 \mu\text{M}$ for the wild type and $150 \pm 25 \mu\text{M}$ for D103A. This is remarkably similar for the two proteins and implies that the D103A mutation does not affect the calcium binding events responsible for the spectral signal change. The

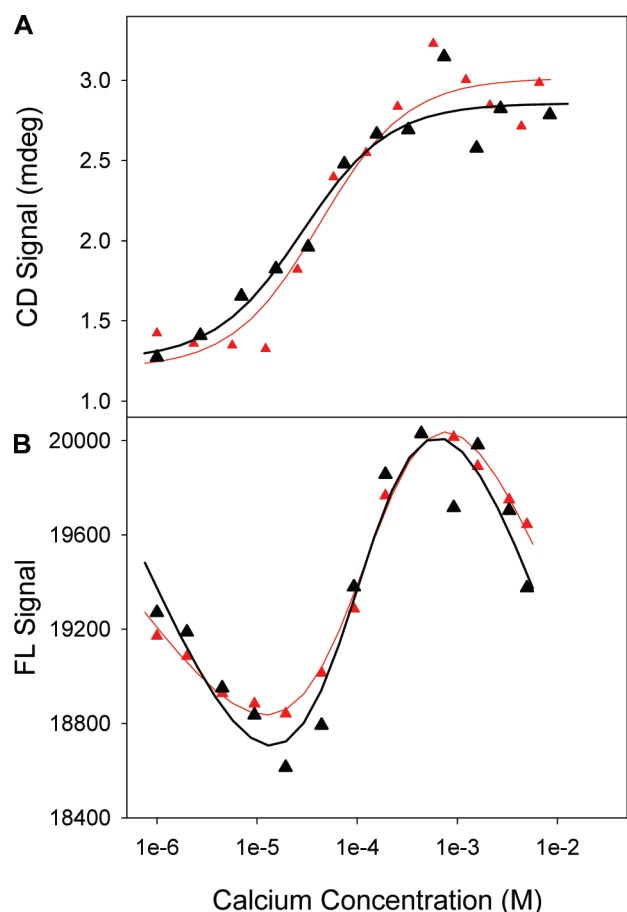


Figure 5. Calcium titrations of the wild type (black) and D103A (red) monitored by (A) CD at 229 nm and (B) FL at an emission wavelength, λ_{em} , of 330 nm. Resolved free energies are listed in Table 2. Curves are simulated on the basis of values resolved from fits to eqs 1 and 2.

calcium binding data for the wild type and D103A fit well to a model with independent sites and showed no evidence of positive cooperativity as judged by inspection of the residuals of the fits. This is surprising given the proximity of the sites and the prevalence of bidentate chelators that link the calcium-binding sites. The small but significant difference in free energy between the calcium titrations monitored by CD and FL may indicate anticooperativity (or heterogeneity) between the sites in the absence of dimerization.

Equilibrium Dialysis Studies. The stoichiometry of calcium binding for both the wild type (WT) and D103A was determined by using equilibrium dialysis with $^{45}\text{Ca}^{2+}$. Data are shown in Figure 6. The stoichiometry of calcium binding was resolved by fitting the data to a model of equal and independent sites as shown in eq 3. This analysis yielded an apparent stoichiometry for calcium binding of 3.3 ± 0.2 for WT and 3.1 ± 0.1 for D103A. Thus, both proteins exhibited a stoichiometry of 3 at high calcium concentrations. This is a critical point for the assembly studies presented subsequently.

To resolve the estimates of calcium binding affinity and cooperativity, we fit the binding data to the Hill equation as shown in eq 4. Fits to the wild-type calcium binding data yielded a Hill coefficient of 1.4 ± 0.1 , demonstrating positive cooperativity with an apparent K_d of $110 \pm 100 \mu\text{M}$. This is a significant increase in cooperativity as compared to that seen in the

Table 2. Summary of Free Energy Changes Resolved from Fits to eq 2^a

protein	CD ΔG° (kcal/mol)	FL ΔG° (kcal/mol)
wild type	-6.2 ± 0.2	-5.4 ± 0.3
D103A	-6.0 ± 0.3	-5.2 ± 0.1

^a Reported errors are either the standard deviation in the average of the best fit value for the parameter, or the largest error in the resolved parameter on an individual fit, whichever is larger.

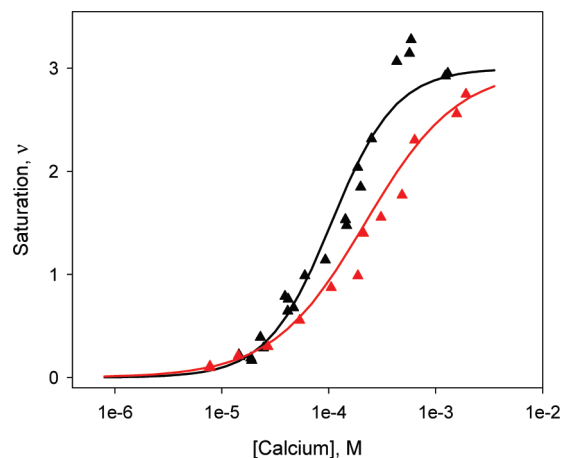


Figure 6. Equilibrium dialysis of the wild type and D103A. The $100 \mu\text{L}$ protein samples of the wild type (black) and D103A (red) were dialyzed against $300 \mu\text{L}$ of buffer containing $^{45}\text{Ca}^{2+}$ ($10 \mu\text{Ci/mL}$) and varying concentrations of unlabeled Ca^{2+} ($0.05\text{--}3 \text{ mM}$). Curves are simulated on the basis of values resolved from fits to eq 4.

spectroscopic studies. One explanation is that the apparent cooperativity increases with dimerization as noted by Alattia et al. for ECAD12³⁵ and illustrated in the simulations presented in the Supporting Information.

Fits to the D103A calcium binding data yielded a Hill coefficient of 0.98 ± 0.03 , demonstrating noncooperativity with an apparent K_d of $250 \pm 90 \mu\text{M}$. These results indicate that the D103A mutation impacted the apparent calcium binding affinity (Figure 6). As noted before, this was not observed in titrations monitored by CD and FL, indicating that these spectral signals are insensitive to the mutation. Our results agree closely with studies of D103A-ECAD12 by Courjean et al. that indicated that three calcium ions bound to this mutant with an apparent K_d of $240 \pm 7 \mu\text{M}$.⁵¹

Assembly Studies. Analytical SEC was performed to monitor dimerization as a function of calcium concentration. Figure 7 illustrates the linkage between calcium binding and dimerization equilibria. If the monomer and dimer are in equilibrium, the relative amount of monomer and dimer in a solution will be dependent upon the concentrations of protein and calcium. All four proteins (wild type, D103A, D134A, and D136N) exhibited two peaks in the SEC chromatograms, which indicates that the dissociation of dimer is slow on the chromatographic time scale ($\sim 30 \text{ min}$). In the apo state, the wild type and the mutants were predominantly in monomeric form (Figure 7, first row). Upon addition of calcium, there was a significant difference in the level of dimer formation between the wild type and mutants. The wild-type data showed that as the calcium concentration increased, the amount of dimer increased (Figure 7A). The dimer fraction in

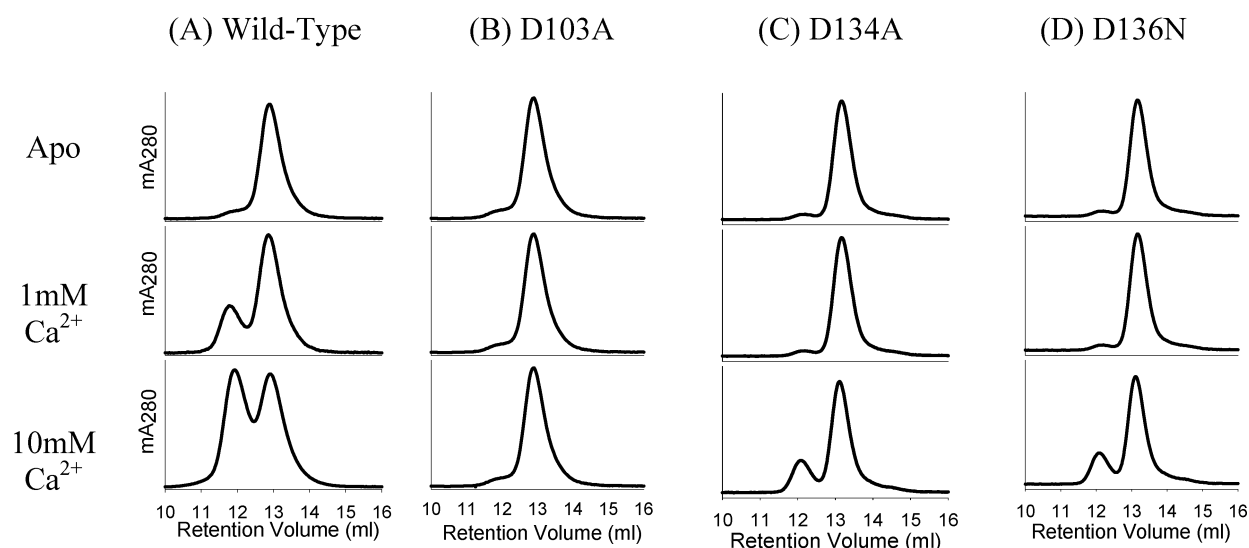


Figure 7. Analytical SEC data illustrating the difference in dimerization as a function of calcium concentration. Protein stocks (50 μM) were injected into the SEC column in the absence (first row) and presence (second and third rows) of calcium for (A) the wild type, (B) D103A, (C) D134A, and (D) D136N. The dimer peak eluted at 11.8 mL and the monomer peak at 13.0 mL.

D134A and D136N was unchanged upon addition of 1 and 5 mM calcium (data not shown). At 10 mM calcium, D134A and D136N exhibited a slight increase in the dimer fraction (Figure 7C,D). These results show that the mutated calcium-binding sites can be occupied if the calcium concentration is 10-fold greater than the physiological level; the mutations at D134 and D136 severely decrease the calcium binding affinity of the protein. In contrast, D103A showed no significant difference in the fraction of dimer upon addition of 10 mM calcium (Figure 7B), even though 10 mM calcium is 10-fold greater than the K_d for site 1 in D103A (Figure 6). Thus, these results indicate that although D103A binds all three calcium ions, it did not form a dimer.

DISCUSSION

Despite the importance of calcium binding in cadherin-mediated cell adhesion, the relative significance of the calcium binding events in dimerization has not been determined previously. We have focused our studies on three critical amino acids, D103, D136, and D134, at the EC1–EC2 interface to elucidate the linkage between the binding of calcium and formation of a dimer in N-cadherin. Figure 8 shows a model for sequential binding of calcium to the EC1–EC2 interface. This model has two main components. First, the binding of calcium is sequential; site 3 must bind first followed by site 2 and then site 1. Second, the physical linkage between site 2 and site 1 provided by D103 is essential for dimerization. This model was developed from studies of each mutant as discussed below.

Sequential Binding of Calcium. D134 provides both of its side chain oxygens to site 3⁵⁴ and has been shown to be important for adhesion.⁵ Our data unequivocally show that a single mutation in site 3, D134A, affects not only the binding of calcium to site 3 but also the binding to site 2 and site 1 in the EC1–EC2 interface (Figure 8). This was demonstrated by spectral, thermal denaturation, and direct calcium titration studies. There was no calcium-dependent change in the CD spectra or in the thermal stability and no calcium binding apparent in the calcium titrations monitored spectroscopically.

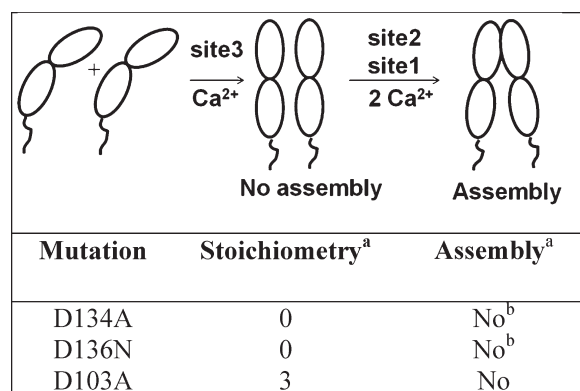


Figure 8. Sequential binding model for calcium binding to the EC1–EC2 interface. The diagram illustrates sequential binding of calcium to site 3, site 2, and site 1 at the EC1–EC2 interface and the summary of the impact of the mutations in calcium-induced dimerization. Calcium binding to site 3 occurs first and is required for binding of calcium to site 2 and then site 1. Assembly requires binding of all three calcium ions and direct linkage between site 2 and site 1 through the side chain oxygens of D103. ^a Observed at physiological calcium concentration (1 mM). ^b Assembly was observed at 10 mM calcium.

These results show that calcium binding to wild-type NCAD12 is sequential; binding at site 3 is required for binding at site 2 and site 1.

The requirement of the occupancy of site 3 for binding of site 2 and site 1 was also supported by our D136N results. We mutated this residue to address the significance of linkage between site 3 and site 2 in dimerization. The mutation of D to N (D136N) was chosen to preserve the carbonyl oxygen for binding of calcium with the expectation that site 3 would still bind calcium. If the calcium binding were not sequential, this mutation would not affect the binding of calcium to site 1. Surprisingly, the D136N mutation severely impaired the binding of calcium at site 3 as demonstrated by a lack of significant change in the CD spectrum or the thermal stability upon addition of calcium. These results

confirm the mandatory occupancy of site 3 for binding of site 2 and site 1. One possible explanation for these results is that the negative charge on D136 is required for binding of calcium to site 3. The importance of preserving opposing negative charges in the chelating residues has been well documented for EF-hand proteins.⁵⁹ Black and co-workers report a 5-fold increase in K_d for calcium caused by removal of a negative charge from site 1 in the N-terminal domain of calmodulin and a 50-fold increase in K_d for Mg^{2+} binding to that same domain.⁶⁰ This decrease in affinity is on the same order of magnitude as that observed in our system for the D136N mutation.

Spectroscopic, equilibrium dialysis, and assembly studies with D103A further strengthen our sequential binding model. Unlike the D134A and D136N mutations, the D103A mutation slightly impacted the calcium binding affinity, yet it has full occupancy of the three calcium-binding sites at physiological calcium concentrations. Because the D134A and D136N mutations (for site 3) completely abolish calcium binding and the D103A mutation (site 1) marginally impacts calcium binding, we confirm unequivocally that the binding at site 3 is required for binding at site 2 and site 1. Our experimental results reach a conclusion identical to that reached by molecular dynamics simulations of calcium binding to the EC1–EC2 interface of E-cadherin by Cailliez et al., which also indicated the requirement of occupancy of site 3 for binding to site 2 and site 1.³⁷

Dimerization Requires Linkage between Site 2 and Site 1. The significance of linkage between site 2 and site 1 in calcium-induced dimerization was demonstrated in equilibrium dialysis and assembly studies with D103A. Equilibrium dialysis experiments demonstrated that all three calcium-binding sites in D103A are saturated at 2 mM calcium. In spite of this, analytical SEC studies showed no dimerization of D103A at 10 mM calcium, thereby indicating the critical importance of the physical connection between site 1 and site 2 that D103 provides. Additional evidence that D103A does not form dimer is the shape of the transitions in the equilibrium dialysis experiments. Here, the protein concentrations exceeded the K_d for dimerization such that for the wild type, as calcium was added, dimer formed. Because of the linkage between the dimerization and calcium binding equilibria, the calcium binding curve appears cooperative regardless of whether calcium binding is intrinsically cooperative (see the Supporting Information). Thus, positive cooperativity was observed for the wild type where dimerization occurs. However, cooperativity was not observed for D103A, supporting the idea that dimerization does not occur. This has been noted previously for ECAD12.³⁵ These results confirm that calcium binding is necessary but not sufficient for dimerization. The physical linkage between site 1 and site 2 provided by D103 is also required for dimerization. This was further supported by analytical SEC studies of D134A and D136N. These mutants showed dimerization at 10 mM calcium. Although D134A and D136N mutations impacted the calcium binding affinity, they still have the linking amino acid (D103) between site 2 and site 1. Because of this linkage, they showed dimerization at 10 mM calcium.

Our studies address the relative significance of calcium-binding sites at the EC1–EC2 interface and allowed us to develop a model for occupancy of the binding sites and formation of the dimer. In summary, our results confirm that calcium binding is sequential such that site 3 must be occupied first and that the linkage between site 1 and site 2 is necessary for the formation of the dimer. N-Cadherin-mediated cell adhesion exerts profound

biological effects during development, in health, and in disease. Hence, it is important to understand the mechanism of cell adhesion by these molecules. Our sequential binding model provides a fundamental understanding of the molecular events leading to cell adhesion by these molecules.

■ ASSOCIATED CONTENT

Supporting Information. A simulation that illustrates the linkage between the apparent binding constant and dimerization. This material is available free of charge via the Internet at <http://pubs.acs.org>.

■ AUTHOR INFORMATION

Corresponding Author

*Department of Chemistry and Biochemistry, University of Mississippi, University, MS 38677. Phone: (662) 915-5328. Fax: (662) 915-7300. E-mail: spedigo@olemiss.edu.

Funding Sources

This work was supported by Grant MCB 0950494 from the National Science Foundation.

■ ABBREVIATIONS

apo, calcium-depleted; CD, circular dichroism; D103A, mutation of aspartate at position 103 to alanine in NCAD12; D134A, mutation of aspartate at position 134 to alanine in NCAD12; D136N, mutation of aspartate at position 136 to asparagine in NCAD12; EC, extracellular domain; EC1, extracellular domain 1 of NCAD12; EC2, extracellular domain 2 of NCAD12; ECAD12, epithelial cadherin domains 1 and 2; EGTA, ethylene glycol tetraacetic acid; FL, fluorescence emission; HEPES, *N*-(2-hydroxyethyl)piperazine-*N'*-2-ethanesulfonic acid; ICP-OES, inductively coupled plasma optical emission spectroscopy; K_d , dissociation constant; NCAD12, neural cadherin domains 1 and 2 (residues 1–221); PDB, Protein Data Bank; SEC, size exclusion chromatography; T_m , melting temperature; wild type, wild-type NCAD12.

■ REFERENCES

- (1) Alattia, J. R., Kurokawa, H., and Ikura, M. (1999) Structural view of cadherin-mediated cell-cell adhesion. *Cell. Mol. Life Sci.* 55, 359–367.
- (2) Ringwald, M., Schuh, R., and Vestweber, D. (1987) et al. The structure of cell adhesion molecule uvomorulin. Insights into the molecular mechanism of Ca^{2+} -dependent cell adhesion. *EMBO J.* 6, 3647–3653.
- (3) Takeichi, M. (1991) Cadherin cell adhesion receptors as a morphogenetic regulator. *Science* 251, 1451–1455.
- (4) Vleminckx, K., and Kemler, R. (1999) Cadherins and tissue formation: Integrating adhesion and signaling. *BioEssays* 21, 211–220.
- (5) Ozawa, M., Engel, J., and Kemler, R. (1990) Single amino acid substitutions in one Ca^{2+} binding site of uvomorulin abolish the adhesive function. *Cell* 63, 1033–1038.
- (6) Yagi, T., and Takeichi, M. (2000) Cadherin superfamily genes: Functions, genomic organization, and neurologic diversity. *Genes Dev.* 14, 1169–1180.
- (7) Chothia, C., and Jones, E. Y. (1997) The molecular structure of cell adhesion molecules. *Annu. Rev. Biochem.* 66, 823–862.
- (8) Gumbiner, B. M. (1996) Cell adhesion: The molecular basis of tissue architecture and morphogenesis. *Cell* 84, 345–357.
- (9) Takeichi, M. (1995) Morphogenetic roles of classic cadherins. *Curr. Opin. Cell Biol.* 7, 619–627.

- (10) Rowlands, T. M., Symonds, J. M., and Farookhi, R. (2000) et al. Cadherins: Crucial regulators of structure and function in reproductive tissues. *Rev. Reprod.* 5, 53–61.
- (11) Gumbiner, B. M. (2005) Regulation of cadherin-mediated adhesion in morphogenesis. *Nat. Rev. Mol. Cell Biol.* 6, 622–634.
- (12) Takeichi, M. (1993) Cadherins in cancer: Implications for invasion and metastasis. *Curr. Opin. Cell Biol.* 5, 806–811.
- (13) Handschuh, G., Candidus, S., and Lubert, B. (1999) et al. Tumour-associated E-cadherin mutations alter cellular morphology, decrease cellular adhesion and increase cellular motility. *Oncogene* 18, 4301–4312.
- (14) Jeanes, A., Gottardi, C. J., and Yap, A. S. (2008) Cadherins and cancer: How does cadherin dysfunction promote tumor progression?. *Oncogene* 27, 6920–6929.
- (15) Yu, X., and Malenka, R. C. (2004) Multiple functions for the cadherin/catenin complex during neuronal development. *Neuropharmacology* 47, 779–786.
- (16) Fannon, A. M., and Colman, D. R. (1996) A model for central synaptic junctional complex formation based on the differential adhesive specificities of the cadherins. *Neuron* 17, 423–434.
- (17) Uchida, N., Honjo, Y., and Johnson, K. R. (1996) et al. The catenin/cadherin adhesion system is localized in synaptic junctions bordering transmitter release zones. *J. Cell Biol.* 135, 767–779.
- (18) Jungling, K., Eulenburg, V., and Moore, R. (2006) et al. N-cadherin transsynaptically regulates short-term plasticity at glutamatergic synapses in embryonic stem cell-derived neurons. *J. Neurosci.* 26, 6968–6978.
- (19) Huntley, G. W., Gil, O., and Bozdagi, O. (2002) The cadherin family of cell adhesion molecules: Multiple roles in synaptic plasticity. *Neuroscientist* 8, 221–233.
- (20) Uemura, T. (1998) The cadherin superfamily at the synapse: More members, more missions. *Cell* 93, 1095–1098.
- (21) Hazan, R. B., Phillips, G. R., and Qiao, R. F. (2000) et al. Exogenous expression of N-cadherin in breast cancer cells induces cell migration, invasion, and metastasis. *J. Cell Biol.* 148, 779–790.
- (22) Nieman, M. T., Prudoff, R. S., and Johnson, K. R. (1999) et al. N-cadherin promotes motility in human breast cancer cells regardless of their E-cadherin expression. *J. Cell Biol.* 147, 631–644.
- (23) Hazan, R. B., Kang, L., and Whooley, B. P. (1997) et al. N-cadherin promotes adhesion between invasive breast cancer cells and the stroma. *Cell Adhes. Commun.* 4, 399–411.
- (24) Nollet, F., Kools, P., and van Roy, F. (2000) Phylogenetic analysis of the cadherin superfamily allows identification of six major subfamilies besides several solitary members. *J. Mol. Biol.* 299, 551–572.
- (25) Pokutta, S., and Weis, W. I. (2007) Structure and mechanism of cadherins and catenins in cell-cell contacts. *Annu. Rev. Cell Dev. Biol.* 23, 237–261.
- (26) Salinas, P. C., and Price, S. R. (2005) Cadherins and catenins in synapse development. *Curr. Opin. Neurobiol.* 15, 73–80.
- (27) Behrens, J. (1999) Cadherins and catenins: Role in signal transduction and tumor progression. *Cancer Metastasis Rev.* 18, 15–30.
- (28) Kemler, R., and Ozawa, M. (1989) Uvomorulin-catenin complex: Cytoplasmic anchorage of a Ca^{2+} -dependent cell adhesion molecule. *BioEssays* 11, 88–91.
- (29) Boggon, T. J., Murray, J., and Chappuis-Flament, S. (2002) et al. C-cadherin ectodomain structure and implications for cell adhesion mechanisms. *Science* 296, 1308–1313.
- (30) Takeichi, M. (1977) Functional correlation between cell adhesive properties and some cell surface proteins. *J. Cell Biol.* 75, 464–474.
- (31) Takeichi, M. (1990) Cadherins: A molecular family important in selective cell-cell adhesion. *Annu. Rev. Biochem.* 59, 237–252.
- (32) Nose, A., Nagafuchi, A., and Takeichi, M. (1988) Expressed recombinant cadherins mediate cell sorting in model systems. *Cell* 54, 993–1001.
- (33) Hynes, R. O. (1999) Cell adhesion: Old and new questions. *Trends Cell Biol.* 9, M33–M37.
- (34) Pokutta, S., Herrenknecht, K., and Kemler, R. (1994) et al. Conformational changes of the recombinant extracellular domain of E-cadherin upon calcium binding. *Eur. J. Biochem.* 223, 1019–1026.
- (35) Alattia, J. R., Ames, J. B., and Porumb, T. (1997) et al. Lateral self-assembly of E-cadherin directed by cooperative calcium binding. *FEBS Lett.* 417, 405–408.
- (36) Prakasam, A., Chien, Y. H., and Maruthamuthu, V. (2006) et al. Calcium site mutations in cadherin: Impact on adhesion and evidence of cooperativity. *Biochemistry* 45, 6930–6939.
- (37) Cailliez, F., and Lavery, R. (2005) Cadherin mechanics and complexation: The importance of calcium binding. *Biophys. J.* 89, 3895–3903.
- (38) Sotomayor, M., and Schulten, K. (2008) The allosteric role of the Ca^{2+} switch in adhesion and elasticity of C-cadherin. *Biophys. J.* 94, 4621–4633.
- (39) Klingelhofer, J., Troyanovsky, R. B., and Laur, O. Y. (2000) et al. Amino-terminal domain of classic cadherins determines the specificity of the adhesive interactions. *J. Cell Sci.* 113 (Part 16), 2829–2836.
- (40) Shan, W., Yagita, Y., and Wang, Z. (2004) et al. The minimal essential unit for cadherin-mediated intercellular adhesion comprises extracellular domains 1 and 2. *J. Biol. Chem.* 279, 55914–55923.
- (41) Overduin, M., Harvey, T. S., and Bagby, S. (1995) et al. Solution structure of the epithelial cadherin domain responsible for selective cell adhesion. *Science* 267, 386–389.
- (42) Haussinger, D., Ahrens, T., and Sass, H. J. (2002) et al. Calcium-dependent homoassociation of E-cadherin by NMR spectroscopy: Changes in mobility, conformation and mapping of contact regions. *J. Mol. Biol.* 324, 823–839.
- (43) Shapiro, L., Fannon, A. M., and Kwong, P. D. (1995) et al. Structural basis of cell-cell adhesion by cadherins [see comments]. *Nature* 374, 327–337.
- (44) Haussinger, D., Ahrens, T., and Aberle, T. (2004) et al. Proteolytic E-cadherin activation followed by solution NMR and X-ray crystallography. *EMBO J.* 23, 1699–1708.
- (45) Parisini, E., Higgins, J. M., and Liu, J. H. (2007) et al. The crystal structure of human E-cadherin domains 1 and 2, and comparison with other cadherins in the context of adhesion mechanism. *J. Mol. Biol.* 373, 401–411.
- (46) Patel, S. D., Ciatto, C., and Chen, C. P. (2006) et al. Type II cadherin ectodomain structures: Implications for classical cadherin specificity. *Cell* 124, 1255–1268.
- (47) Harrison, O. J., Corps, E. M., and Berge, T. (2005) et al. The mechanism of cell adhesion by classical cadherins: The role of domain 1. *J. Cell Sci.* 118, 711–721.
- (48) Handschuh, G., Lubert, B., and Hutzler, P. (2001) et al. Single amino acid substitutions in conserved extracellular domains of E-cadherin differ in their functional consequences. *J. Mol. Biol.* 314, 445–454.
- (49) Klingelhofer, J., Laur, O. Y., and Troyanovsky, R. B. (2002) et al. Dynamic interplay between adhesive and lateral E-cadherin dimers. *Mol. Cell Biol.* 22, 7449–7458.
- (50) Koch, A. W., Pokutta, S., and Lustig, A. (1997) et al. Calcium binding and homoassociation of E-cadherin domains. *Biochemistry* 36, 7697–7705.
- (51) Courjean, O., Chevreux, G., and Perret, E. (2008) et al. Modulation of E-cadherin monomer folding by cooperative binding of calcium ions. *Biochemistry* 47, 2339–2349.
- (52) Corps, E., Carter, C., and Karecla, P. (2001) et al. Recognition of E-cadherin by integrin $\alpha_E\beta_7$: Requirement for cadherin dimerization and implications for cadherin and integrin function. *J. Biol. Chem.* 276, 30862–30870.
- (53) Pertz, O., Bozic, D., and Koch, A. W. (1999) et al. A new crystal structure, Ca^{2+} dependence and mutational analysis reveal molecular details of E-cadherin homoassociation. *EMBO J.* 18, 1738–1747.
- (54) Nagar, B., Overduin, M., and Ikura, M. (1996) et al. Structural basis of calcium-induced E-cadherin rigidification and dimerization. *Nature* 380, 360–364.

(55) Pace, C. N., Vajdos, F., and Fee, L. (1995) et al. How to measure and predict the molar extinction coefficient of a protein. *Protein Sci.* 4, 2411–2423.

(56) Prasad, A., Housley, N. A., and Pedigo, S. (2004) Thermodynamic stability of domain 2 of epithelial cadherin. *Biochemistry* 43, 8055–8066.

(57) García De La Torre, J., Huertas, M. L., and Carrasco, B. (2000) Calculation of hydrodynamic properties of globular proteins from their atomic-level structure. *Biophys. J.* 78, 719–730.

(58) Greenfield, N., and Fasman, G. D. (1969) Computed circular dichroism spectra for the evaluation of protein conformation. *Biochemistry* 8, 4108–4116.

(59) Black, D. J., Tikunova, S. B., and Johnson, J. D. (2000) et al. Acid pairs increase the N-terminal Ca^{2+} affinity of CaM by increasing the rate of Ca^{2+} association. *Biochemistry* 39, 13831–13837.

(60) Tikunova, S. B., Black, D. J., and Johnson, J. D. (2001) et al. Modifying Mg^{2+} binding and exchange with the N-terminal of calmodulin. *Biochemistry* 40, 3348–3353.